arXiv:cond-mat/9908127v4 [cond-mat.stat-mech] 14 Dec 2000

Synchronization of non-chaotic dynamical systems

Franco Bagnoli [a,c,*] Fabio Cecconi [b,d]

[a] *Dipartimento di Matematica Applicata, Università di Firenze, Via S. Marta, 3 I-50139 Firenze*

[b] *International School for Advanced Studies (SISSA/ISAS) via Beirut 2-4, I-34014 Trieste*

[c] *INFM Unità di Ricerca di Firenze*

[d] *INFM Unità di Ricerca di Trieste (Sissa)*

Abstract

A synchronization mechanism driven by annealed noise is studied for two replicas of a coupled-map lattice which exhibits *stable chaos* (SC), i.e. irregular behavior despite a negative Lyapunov spectrum. We show that the observed synchronization transition, on changing the strength of the stochastic coupling between replicas, belongs to the directed percolation universality class. This result is consistent with the behavior of *chaotic* deterministic cellular automata (DCA), supporting the equivalence Ansatz between SC models and DCA. The coupling threshold above which the two system replicas synchronize is strictly related to the propagation velocity of perturbations in the system.

Key words: transient chaos, stable chaos, synchronization, cellular automata
PACS: 05.45.+b, 05.40.+J, 05.70.Jk

* to whom correspondence should be addressed
Email addresses: bagnoli@dma.unifi.it (Franco Bagnoli), cecconi@sissa.it (Fabio

1 Introduction

The occurrence of disordered patterns and their propagation in the presence of a negative Lyapunov spectrum have been often observed in spatiotemporal systems [1–5]. One can classify this kind of irregular behavior into two general groups with basically different features: *transient chaos* and *stable chaos*.

Transient chaos (TC) is a truly chaotic regime with finite lifetime, characterized by the coexistence in the phase space of stable attractors and chaotic non attracting sets - named chaotic saddles or repellers [6]. The system, starting from a generic configuration, typically exhibits irregular behavior until it collapses abruptly onto a nonchaotic attractor.

Stable chaos (SC) constitutes a different kind of transient irregular behavior [1,2] which cannot be ascribed to the presence of chaotic saddles and therefore to divergence of nearby trajectories. In SC systems, moreover, the time spent in transient regimes may scale exponentially with the system size (supertransients [1,2]), and the final stable attractor is practically never reached for large enough systems. One is thus allowed to assume that such transients may be of substantial experimental interest and become the only physically relevant states in the thermodynamic limit. While TC remains associated to information production, i.e. to the response of the system to infinitesimal disturbances, SC is mainly related to propagation and mixing of information. In other words, SC systems are sensitive only to perturbations of finite amplitude [7], while they respond to infinitesimal disturbances in a way similar to stable systems. Such a key feature makes meaningless any characterization of the SC complexity by means of Lyapunov theory.

In this paper we focus on SC behavior whose origin has not yet found a convincing explanation, even though, it has been observed in several spatially-

Cecconi).

extended models such as coupled map lattices [1–3] and oscillators [4]. To provide an adequate description of SC systems we invoke their strict similarity with discrete models such as deterministic cellular automata (DCA). In fact, according to the conjecture that "SC systems represent a continuous generalization of deterministic cellular automata" [2], we can argue that, what is known about DCA could be automatically translated into the language of SC. Although a general mapping of SC- onto DCA-models is still missing, the conjecture is supported by the fact that, also in finite size DCA, limit cycles and fixed points are the only allowed attractors, since the number of possible configurations is finite. Moreover in some DCA, the transient dynamics towards the final attractor may exhibits a long living irregular behavior with lifetimes that typically grow exponentially with the system size. In this case it is practically impossible to find any recurrence (Poincaré cycles) for large systems. According to Wolfram classification [8], these DCA form the third ("chaotic") class and they share several properties with continuous SC systems.

The emergence of this "chaoticity" in DCA dynamics, is effectively illustrated by the damage spreading analysis [9,10], which measures the sensitivity to initial conditions and for this reason is considered as the natural extension of the Lyapunov technique to discrete systems. In this method, indeed, one monitors the behavior of the distance between two replicas of the system evolving from slightly different initial conditions. The dynamics is considered unstable and the DCA is said chaotic, whenever a small initial difference between replicas spreads through the whole system. On the contrary, if the initial difference eventually freezes or disappears, the DCA is considered non chaotic.

A similar scenario holds for systems exhibiting SC [3], where a transitions between regular and irregular dynamics may occur upon changing a control parameter (e.g. the spatial coupling between sites); the irregular dynamics is

often associated to spreading of damages.

In this work we show that another characterization of the SC behavior can be achieved through a suitable synchronization method, which has been successfully employed in Ref. [11] to classify the chaotic properties of DCA. In our opinion this method may be used to complement the common damage spreading analysis. The basic idea consists of measuring the minimal "strength" of the coupling between a replica (slave) and the original system (master) required to achieve their perfect synchronization. The master-slave interaction is a stochastic and spatially-extended version of the Pecora-Carroll synchronization mechanism [12]. Unlike the damage spreading method, where replicas are independent, this coupling scheme implies that the evolution of slave is driven by the master. Practically each time step is composed by two phases: in the first one, the master and slave system evolve freely with the same evolution equation, and then a fraction p of the degrees of freedom in the slave-system is enforced to take the value of the corresponding degrees of freedom in the master. Synchronization of spatially extended systems has been usually studied with symmetrical interactions [13–17]. Our asymmetric scheme, instead, allows probing the dynamical properties of the master system. Through a gradual increase of p from 0 to 1, the dynamics of the slave system tends to synchronize to that of master, and at a threshold p^* a synchronization transition occurs: the pinching synchronization transition (PST). The threshold p^* above which the replicas synchronize, is an indicator of the chaotic behavior of the unperturbed system (master). Indeed, a large value of p^* implies a large fraction of sites to be pinched in order to achieve the synchronization, indicating that the dynamics of the replicas is rather irregular and difficult to control.

In DCA, the PST belongs to the directed percolation (DP) universality class [11,17], while in fully chaotic continuous systems (e.g. coupled map lattices) the synchronization is never perfect for finite times, nor it is equivalent to an absorbing

state [17]. This generally implies non-DP scaling exponents [18–20]. Here, we find that the PST is well defined for a model showing typical SC behavior originally introduced in Ref. [2]. This PST is found to belong to the DP universality class, in agreement to what happens for DCAs. The result further supports the conjecture that SC class contains DCAs.

The sketch of this paper is the following. In the next section, we study a simple coupled-map lattice which is particularly suitable for discussing the distinction between SC and TC behaviour. The model, in fact, displays a TC regime before falling into DCA dynamics with the typical properties of a discrete SC regime. In Section III, we describe the SC model of Ref. [2], whose dynamics never reduces to a DCA, and the pinching synchronization technique applied to it. For the latter model we obtain the PST phase diagram (Sec. IV), by measuring the synchronization threshold as a function of the coupling strength between sites. Such a phase diagram agrees remarkably with that already obtained through damage spreading analysis in Ref. [3]. We provide an argument to explain this consistency. Finally, conclusions and remarks are reported in the last section.

2 Transient and stable chaos

It is instructive to discuss the main differences between SC and TC regimes with the aid of a simple spatiotemporal model in which both of them occur.

Let us consider the one-dimensional coupled-map lattice (CML), i.e. an array of state variables $\{x_1, ..., x_L\}$ in the interval $[0, 1]$ subject to the discrete-time evolution rule

$$x_i(t+1) = g_\varepsilon(x_{i-1}(t), x_i(t), x_{i+1}(t)). \tag{1}$$

Each site-variable x_i interacts diffusively with its nearest neighbors

$$g_\varepsilon(u,v,z) = (1-2\varepsilon)f(v) + \varepsilon\Big[f(u)+f(z)\Big]. \tag{2}$$

where ε sets the coupling strength among maps.

The local mapping has the form shown in Fig. 1:

$$f(x) = \begin{cases} 0 & \text{for } 0 \le x < \alpha, \\ \dfrac{x-\alpha}{1/3-2\alpha} & \text{for } \alpha \le x < 1/3-\alpha, \\ 1 & \text{for } 1/3-\alpha \le x < 1/3+\alpha, \\ 1-\dfrac{x-1/3-\alpha}{1/3-2\alpha} & \text{for } 1/3+\alpha \le x < 2/3-\alpha, \\ 0 & \text{for } 2/3-\alpha \le x < 2/3+\alpha, \\ \dfrac{x-2/3-\alpha}{1/3-2\alpha} & \text{for } 2/3+\alpha \le x < 1-\alpha, \\ 1 & \text{for } 1-\alpha \le x < 1. \end{cases} \tag{3}$$

In this example, we always use the democratic coupling $\varepsilon = 1/3$, and we shall neglect to indicate the ε dependence. A typical grayscale pattern generated by the evolution of the above CML is shown in Fig. 2 (see the caption for the grayscale-code), for $\alpha = 0.068$. Note that the continuous dynamics (gray) is limited to restricted domains, while in the rest, the system has fallen into a Boolean dynamics (typical of DCA), which is however far from being trivial.

Systems showing SC and TC regimes are asymptotically stable, therefore the standard Lyapunov spectrum is not able to detect their transiently irregular states. In TC regimes, however, the existence of chaotic saddles in the phase space is revealed by the finite-time (or effective) Lyapunov exponent

$$\gamma(t) = \frac{1}{t}\langle \log \|\mathbf{w}(t)\| \rangle, \tag{4}$$

where $\mathbf{w}(t) = \{w_1(t), ..., w_L(t)\}$ indicates a generic infinitesimal perturbation (i.e., a tangent vector) at time t, which evolves following the linearization of Eqs. (1–3). The average in expression (4) is taken over the ensemble of

trajectories which have not yet left a certain neighborhood of the saddle at time t [21]. The indicator $\gamma(t)$ is expected to fluctuate around a positive value during the transient [5] and switches to negative values after the transition to the stable attractor occurs. In SC, however, even the finite-time Lyapunov exponent does not provide much information, as it becomes negative already in the transients. This indicates that the source of the SC behaviour cannot rely on the instability associated to repelling sets. Although, the existence of repellers may not be excluded *a priori*, certainly their role is not observable in SC.

We now see how the above considerations apply to our toy-model. First, we discuss the case of infinite slope map, (i.e. $\alpha = 1/6$, full line in Fig. 1) corresponding to a pure SC regime. In fact, after one time step, each configuration of the lattice reduces to a sequence of "0" and "1" (Boolean configuration). The system evolution remains, however, irregular since, when $\alpha = 1/6$, the model is equivalent to a DCA which follows the *rule 150*

$$g(u, v, z) = u + v + z - 2(uv + uz + vz) + 4uvz$$

with u,v and z Boolean variables. This dynamics is known to generate highly irregular patterns [8]. On the other hand, this irregular behaviour cannot be associated to either chaotic saddles or local fluctuations of Lyapunov exponent, the latter being $-\infty$ due to the specific form of the map. Despite Lyapunov analysis ensures that this system is totally insensitive to infinitesimal perturbations, finite perturbations of amplitude greater than 1/6 give rise to a "defect" which propagates through the lattice. Indeed, it can be easily shown that a defect also evolves with the chaotic *rule 150*, because the rule is additive modulo two.

A slight tilting of the vertical edges of the map, ($0 < \alpha < 1/6$, dotted and dashed lines in Fig. 1) introduces some expanding regions in the phase space. Accordingly, one obtains a typical TC behaviour, due to the competition be-

tween stable and unstable effects, which decays into the above mentioned SC regime (see Fig. 2). Figure 3 shows a typical time fluctuation of the local expansion rate (or local multiplier) $\mu(t) = \|\mathbf{w}(t)\|/\|\mathbf{w}(t-1)\|$, for $\alpha = 0.052$, $\mathbf{w}$ being a tangent vector as in Eq. (eq:lyap). The irregularity of the signal is a clear indication of the chaotic-like behavior of the system. The simulation is stopped at time T_r when $\mathbf{w}(t)$ becomes exactly $\mathbf{0}$, i.e., when the system settles down into a Boolean configuration (SC state) which is Lyapunov-stable by definition. Therefore, T_r provides an estimate of the time spent in the TC regime.

For all those trajectories which have not yet entered binary configurations at time t, $\gamma(t)$ remains positive, as seen in Fig. 4, where the distribution of $\gamma(t)$ is shown for a set of 2000 trajectories starting from arbitrary initial conditions.

The lifetime T_r of the TC regimes preceding the SC behavior depends on α. T_r becomes shorter as α approaches $1/6$, value at which it vanishes, because the system behaves as a true DCA after just one time step. In the limit $\alpha \to 0$, instead, the flat regions of the map disappear (the slope being equal to 3) and TC regime becomes persistent and degenerates into fully developed chaos (FDC).

A more detailed analysis of the behavior of the model of Eqs. (1–3) upon changing the control parameter α will be presented elsewhere. Here such a qualitative discussion has the only aim to highlight the key differences between SC and TC dynamics, both present in this toy model.

In the example discussed so far, the SC regime occurs only as a DCA behavior, since, as soon as the system falls into a Boolean configuration, it evolves as a genuine "chaotic" DCA. In the following section we discuss a continuous SC model whose behavior never reduces to DCA dynamics. In particular we study the synchronization properties of two replicas of such a system.

3 The model and the synchronization dynamics

The dynamical system considered now, is the one-dimensional CML of Eqs. (1,2) with the coupling constant $\varepsilon \in [0, 1/2]$ and periodic boundary conditions over a length L (system size). The local mapping has the form

$$f(x) = \begin{cases} bx & \text{if } 0 < x < 1/b \\ a + c(x - 1/b) & \text{if } 1/b < x < 1 \end{cases} \tag{5}$$

as shown in Fig. 5.

We use here the parameter values $(a = 0.07,\ b = 2.70,\ c = 0.10)$ of Ref. [3] for which the map of Eq. (5) is attracted into a stable period-3 orbit. An example of the space-time evolution of the CML is shown in Fig. 6, where the presence of propagating structures similar to those in Fig. 2 is observed, despite here the system dynamics never relaxes onto a pure DCA state.

In Ref. [3] an ε-dependent dynamical phase transition between periodic and chaotic regimes of this system has been carefully investigated by damage spreading analysis. The periodic (chaotic) phase is characterized by the absence (presence) of damage propagation which is found to behave linearly

$$S(t) = S(0) + 2V_F t \tag{6}$$

being S the linear size of the region affected by the damage. The factor 2 is a consequence of the symmetric coupling scheme which requires the left and right damage-front to progress at the same velocity V_F, but in opposite directions. The damage spreading velocity V_F can be considered a good indicator for this transition, because it vanishes in periodic phases. It turns out from Ref. [3], that for $\varepsilon < \varepsilon_c^{(1)} \simeq 0.3$ only periodic phases are observed, for $\varepsilon > \varepsilon_c^{(2)} \simeq 0.3005$ only chaotic states exist. In the intermediate region $\varepsilon \in [\varepsilon_c^{(1)}, \varepsilon_c^{(2)}]$, periodic and chaotic behaviors alternate in an apparently irregular manner (fuzzy region).

We study the effects of the pinching synchronization on this model, and its interplay with the above described transition.

The master system follows the dynamics of Eq. (1), while the slave system evolves as

$$y_i(t+1) = [1 - r_i(t)]g_\varepsilon(y_{i-1}(t), y_i(t), y_{i+1}(t)) + r_i(t)g_\varepsilon(x_{i-1}(t), x_i(t), x_{i+1}(t)) \tag{7}$$

where $r_i(t)$ is a Boolean random variable

$$r_i(t) = \begin{cases} 1 & \text{with probability } p, \\ 0 & \text{otherwise.} \end{cases}$$

Practically, at each time step, a fraction p of site variables in the slave system is set equal to the corresponding variables of the master (see. Fig. 7). In the limit case $p = 0$, the slave system evolves independently of the master, while for $p = 1$, its evolution coincides with the master one.

The synchronization order-parameter is the asymptotic value of the topological distance ρ between master and slave systems (i.e. the fraction of non synchronized sites)

$$\rho(t, p) = \lim_{L\to\infty} \frac{1}{L} \sum_{i=1}^{L} \Theta(|x_i(t) - y_i(t)|) \tag{8}$$

where $\Theta(s)$ is the unitary step-function. We denote by p^* the synchronization threshold, such that $\rho(\infty, p < p^*) > 0$ and $\rho(\infty, p < p^*) = 0$. This synchronization mechanism defines an associated directed site-percolation problem in $d = 1 + 1$ dimension, where a site of coordinate (i, t) is "wet" if $r_i(t) = 0$ and it is connected to at least one neighboring wet site at time $t - 1$. At $t = 0$ all sites are assumed to be wet. We denote by p_c the critical threshold for which a cluster of wet sites percolates along the time direction. The master and the slave systems can stay different only on the cluster of wet sites.

For chaotic CMLs two synchronization scenarios are possible, called *weak* and *strong* chaos respectively [22]. A system is said strongly chaotic if it does not synchronize even on the critical wet cluster (i.e. for $p^* = p_c$) and therefore the distance ρ of Eq. (8) always exhibits DP scaling. Alternatively one can say that for strongly chaotic systems, the active and the wet clusters are essentially the same for every value of p.

Instead, for weakly chaotic systems, the synchronization threshold p^* is always located below p_c and the transition is discontinuous (first-order like). For $p < p^*$ again the active and wet clusters coincide, whereas for $p > p^*$ the active cluster disappears, but the wet cluster still percolates. Such a behavior is due to the exponential vanishing of the difference field $\mathbf{h}(t) = \{x_i(t) - y_i(t)\}_{i=1}^{L}$, even though local fluctuations of $\mathbf{h}$ can sporadically appear.

However, for chaotic systems, the synchronized state is not robust with respect to an infinitesimal perturbation in the absence of the synchronization mechanism, i.e. it is not a proper absorbing state. Conversely, DCAs [11] always synchronize at p^* below p_c (i.e. synchronization occurs in presence of the percolating wet cluster) but $\rho(t, p)$ still exhibits DP scaling. This is a straightforward consequence of the finiteness of the number of states in DCAs, which prevents fluctuations of $\mathbf{h}$ in the absorbing state. The toy model of Section II trivially follows this behavior, and the synchronized state is insensitive with respect to sufficiently small perturbations. We show in the following that this scenario holds also for continuous SC systems.

4 Numerical results

A first set of simulations has been performed for lattices of size $L = 3000$, with periodic boundary conditions. We measured $\rho(t, p)$ at different times and the results have been averaged over a 5000 randomly chosen initial conditions.

For each simulation a transient of 10^4 time steps has been discarded in order to avoid initial bias and reach stationary states. A site i is considered to be synchronized (and $y_i(t+1)$ is set equal to $x_i(t+1)$) if $|y_i(t) - x_i(t)| < \tau$, where τ is a sensibility threshold. In this way we can control the effects of the finite precision of computer numbers. We checked that the results are independent of τ (for small τ), and we choose $\tau = 10^{-8}$ for massive simulations.

A typical behavior of $\rho(t, p)$ near p^* is shown in Fig. 8. The value of p corresponding to the most straight curve at large t represents the best approximation of p^*, which can be estimated with good accuracy. The straight dashed line indicates the DP scaling results.

For those values of ε for which the above analysis provided a too uncertain result in the estimation of p^*, we have carried out single-site simulations for larger systems, obtaining a more accurate determination of p^*. These simulations consist in preparing the slave system exactly synchronized to the master except for the central site, and in measuring how non-synchronized sites propagate throughout the system, generating DP-like clusters. This method probes the stability of synchronized states with respect to minimal perturbations.

As usual in this type of simulations, we measured the survival probability $P(t)$ of the desynchronized states, the number of non synchronized sites $N(t)$, and their second moment $R^2(t)$ with respect to the center of the lattice (generally called the gyration radius). Near the synchronization threshold and in the long time limit, these magnitudes are expected to scale as [23,24]

$$N(t) \sim t^{\eta}, \quad P(t) \sim t^{-\delta}, \quad R^2(t) \sim t^{z}. \tag{9}$$

The determination of the asymptotic value of such exponents (e.g. η) is performed by plotting the effective exponent

$$\overline{\eta}(t) = \frac{\log(N(at))}{\log(N(t))}$$

versus $1/t$ for several values of p. Here a indicates an arbitrary scale factor and we always set $a = 2$. In the limit $t \to \infty$ $\overline{\eta}$ converges to η for $p = p^*$, and diverges for other values of p. In pure DP systems this method allows the simulation of effectively infinite lattices, since the reference state, i.e. the absorbing one (usually made of "0"s) is unique and does not change in time. Conversely, in our case the absorbing state coincides with the synchronized state and this implies the detailed knowledge of the evolution of the master system. This circumstance imposes severe limitations on lattice sizes and performances of the method.

In Figure 9 we report the behavior of the effective exponents $\overline{\eta}$, $\overline{\delta}$ and $\overline{z} + \overline{\eta}$ versus $1/t$ for several values of p. The asymptotic values of the exponents ($\eta = 0.330(5)$, $\delta = 0.13(2)$, $z = 1.25(2)$) are consistent with the best known DP ones ($\eta = 0.31368(4)$, $\delta = 0.15947(3)$, $z = 1.26523(3)$ [24]).

This analysis, repeated for several values of ε, indicates that the synchronization of SC systems reasonably belongs to the DP universality class. The very slow convergence of the system dynamics to the asymptotic state makes hard to exclude that for some values of ε the DP character of the transition is violated. However, we believe that, owing to the stability of the model of Eqs. (1,2,3), small local disturbances are re-absorbed at exponential rate, and cannot generate desynchronization effects. In other words, the synchronized state is absorbing with respect to small fluctuations. This is also consistent with the fact that the simulation results are independent of the precision threshold τ. Therefore, the local stability guarantees that, for what concerns synchronization properties, SC systems behave mainly like discrete ones and differently from continuous chaotic systems. This further supports the "*equivalence Ansatz*" between SC and DCA. Indeed, preliminary simulations show that the DP scenario holds even if the local pinching is performed only up to a small difference Δ. This remark suggests the possibility of defining a finite-size maximum Lyapunov exponent, in a way similar to Ref. [25]. Further work in

this direction is in progress.

Finally, the PST phase diagram is shown in Fig. 10, where p^* is plotted versus ε. The behavior of p^* is compared with that of the damage spreading velocity V_F (Ref [3]), properly re-scaled. The consistency of the two phase diagrams, even in the fuzzy region, suggests that the indicators, V_F and p^*, characterize different aspects of the same phenomenon. The strict correlation between V_F and p^* is not surprising if one considers the changing rate of the density of non synchronized sites, $n(t) = N(t)/L$, in the pinching synchronization mechanism. For large time and systems and in a mean-field description of the process, we can write for $n(t)$ an equation similar to that one employed in contact processes and DP theory [26],

$$\dot{n} = 2V_F n(1-n) - pn \; . \tag{10}$$

The first term of the r.h.s. represents the active-site production due to the linear spreading of desynchronization regions, which occurs with a velocity V_F (see Eq. 6)). The second term accounts for the destruction of active sites by the pinching mechanism. The process becomes critical when the linear contributions, $2V_F\, n$ and $p\, n$ balance, thus we obtain $p^* \sim V_F$. The proportionality holds even outside of mean-field approach, i.e., when other terms, such as, higher powers of n, diffusion and multiplicative noise, are included in Eq. (10), provided one considers the renormalized parameters. The conclusion that p^* is a nondecreasing function of V_F is however intuitive, because the higher V_F, the grater is the desynchronization rate, so the pinching probability has to be large to ensure the synchronization.

5 Conclusions

In summary, we have applied the pinching synchronization method to systems showing stable chaos. As for cellular automata, we have found that even in

this continuous case the pinching synchronization transition (PST) is well defined, and that this transition belongs to the DP universality class. Our results show that the stable chaos is indeed equivalent to cellular automata "chaoticity" and definitively different from transient chaos. The PST phase diagram is consistent with that reported in Ref. [3] for damage spreading velocities, including the fuzzy region.

Acknowledgements

We thank A. Politi, R. Livi, A. Vespignani and A. Flammini for fruitful discussions. We also thank all the components of the D.O.C.S. research group of Firenze (http://www.docs.unifi.it) for stimulating discussions and interactions.

References

[1] J.P. Crutchfield and K. Kaneko, Phys. Rev. Lett. **60**, 2715 (1988), K. Kaneko, Phys. Lett. **149A**, 105 (1990).

[2] A. Politi, R. Livi, G.-L. Oppo, and R. Kapral, Europhys. Lett. **22**, 571 (1993).

[3] F. Cecconi, R. Livi and A. Politi, Phys. Rev. E **57**, 2703 (1998).

[4] R. Bonaccini and A. Politi, Physica D **103**, 362 (1997).

[5] Y-C Lai and R.L. Winslow, Phys. Rev. Lett **74**, 5208 (1995).

[6] T. Tel, *Proceedings of the 19th IUPAP International Conference on Statistical Physics*, edited by Hao Bai-lin (World Scientific Publishing: Singapore 1996) *Directions in Chaos*, vol.**3**, edited by Hao Bai-lin (World Scientific Publishing: Singapore 1990)

[7] A. Politi and A. Torcini, Europhys. Lett. **28**, 545 (1994).

[8] S. Wolfram, Rev. Mod. Phys. **55**, 601 (1983).
S. Wolfram (editor), *Theory and Application of Cellular Automata* (World Scientific, Singapore, 1986).

[9] P. Grassberger, J. Stat. Phys. **79**, 13 (1995).

[10] F. Bagnoli, J. Stat. Phys. **79**, 151 (1996).

[11] F. Bagnoli and R. Rechtman, Phys. Rev. E **59**, R1307 (1999).

[12] L.M. Pecora and T.L. Carroll, Phys. Rev. Lett. **64**, 821 (1990).

[13] A. Maritan and J.R. Banavar, Phys. Rev. Lett. **72**, 1451 (1994).

[14] D.H. Zanette and A.S. Mikhailov, Phys Rev. E **58**, 872 (1998).

[15] L.G. Morelli and D.H. Zanette, Phys Rev. E **58**, R8 (1998).

[16] F.S. de San Roman, S. Boccaletti, D. Masa and H. Mancini, Phys. Rev. Lett. **81**, 3639 (1998).

[17] P. Grassberger, Phys. Rev. E **59**, R2520 (1999).

[18] P. Grassberger, in *Proceedings of 1995 Shimla Conference on Complex Systems*, edited by S. Puri *et al.* (Narosa Publishing, New Delhi, 1997).

[19] A.S. Pikovsky and J. Kurths, Phys. Rev. E **49**, 898 (1994).

[20] G. Grinstein, M.A. Muñoz and Y. Tu, Phys. Rev. Lett. **76**, 4376 (1996).

[21] E. Ott, *Chaos in dynamical systems* (Cambridge University Press: Cambridge UK 1993).

[22] F. Bagnoli, L. Baroni, and P. Palmerini, Phys Rev. E **59**, 409 (1999).

[23] P. Grassberger and A. de la Torre, Ann. Phys. (N.Y.) **122**, 373 (1979).

[24] M.A. Mugnoz, R. Dickman, A. Vespignani and S. Zapperi, Phys Rev. E **59**, 6175 (1999).

[25] F. Bagnoli, R. Rechtman and S. Ruffo, Phys. Lett. A **172**, 34 (1992).

[26] H.K. Jannsen, Z. Phys. **B 42**, 151 (1981).

Figure captions

Figure 1: Plot of the map of Eq. (3) for different values of α: $\alpha = 0.02$ (dotted line), $\alpha = 0.08$ (dashed line) and $\alpha = 1/6$ (continuous line).

Figure 2: Grayscale representation of space-time evolution of model of Eq. (2) with $\varepsilon = 1/3$ and $\alpha = 0.068$. Time runs from top to bottom, white (black) color indicates $x_i(t) = 0$ ($x_i(t) = 1$), while gray indicates all other values.

Figure 3: Time behaviour of Lyapunov multiplier $\mu(t) = |\mathbf{z}(t)|/|\mathbf{z}(t-1)|$ for CML of Eq. (2) with $\alpha = 0.052$. The simulation is stopped at time $T_r = 4455$ when the systems reaches the absorbing SC state.

Figure 4: Histogram of the finite-time Lypunov exponent γ of model of Eq. (2) computed from a set of 2000 arbitrary initial conditions, with $\alpha = 0.052$. The size of the system is $L = 3000$ sites. For each initial condition, the evolution of Eq. (2) and its linearization are iterated untill the system approaches a Boolean configuration.

Figure 5: Plot of the map of Eq. (5).

Figure 6: Space-time evolution of the map Eq. 5, with $\varepsilon = 0.32$. Grayscale from $x_i(t) = 0$ (white) to $x_i(t) = 1$ (black).

Figure 7: Schematic representation of the pinching synchronization. Vertical dashed lines indicate the sites of the slave system identified to those of the master corresponding to $r_i = 1$ in Eq. (7).

Figure 8: Log-log plot of the order parameter $\rho(t, p)$ vs. t, for $p = 0.1269, 0.1270, 0.1271...$ from top to down, and for $\varepsilon = 0.305$. The dot-dashed straight line indicates the critical DP scaling $t^{-\delta}$ with $\delta = 0.159$. The estimated synchronization threshold turns to be $p^* = 0.1272(1)$.

Figure 9: effective exponents $\overline{\eta}(t)$ (a), $\overline{\delta}(t)$ (b) and $\overline{z}(t) + \overline{\eta}(t)$ (c) for $\varepsilon = 0.3004$ and several values of p. The average is taken over 50.000 runs, $a = 2$ and $L = 2000$.

Figure 10: Dependence of the synchronization threshold p^* on the coupling constant ε (diamonds) compared with the behaviour of V_F (open circles), the V_F-values are properly re-scaled. In the inset an enlargement of the region around $\varepsilon = 0.3$ is shown. The line is a guide to eye.

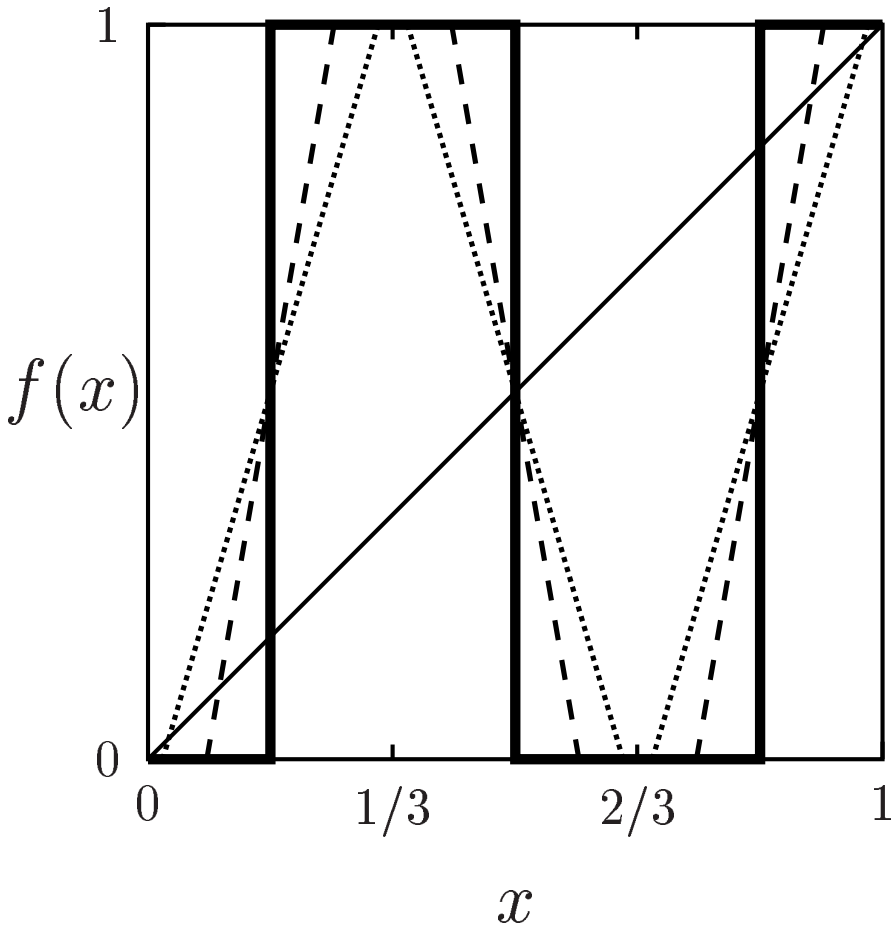

Bagnoli and Cecconi, *Synchronization of non-chaotic ...* Figure 1

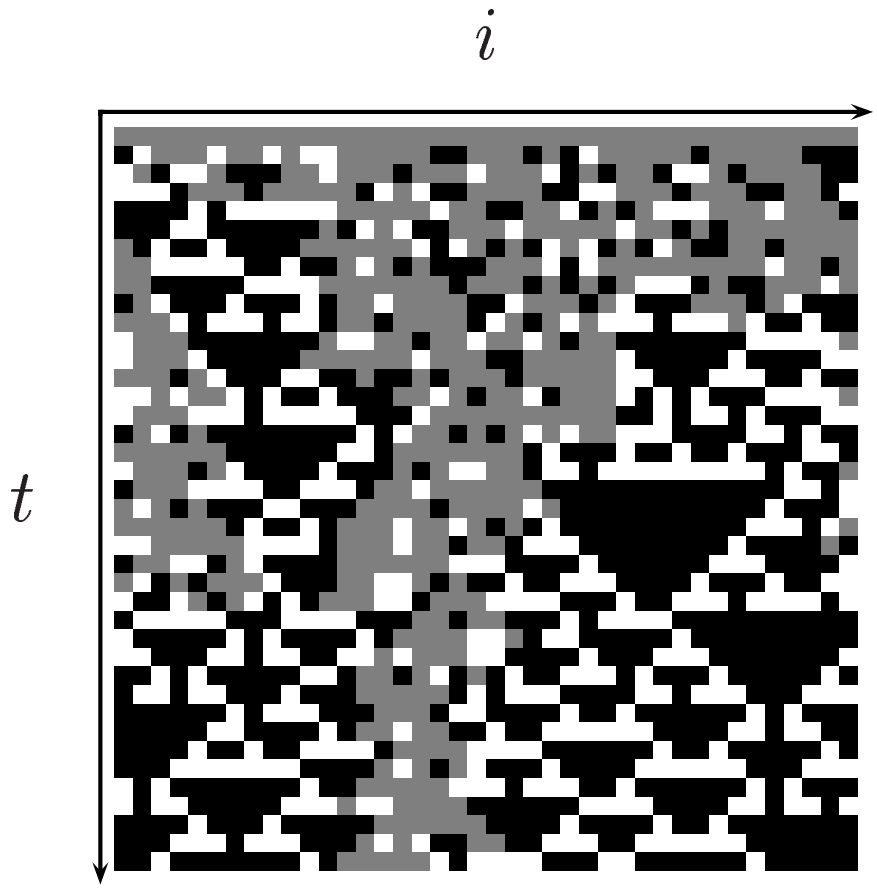

Bagnoli and Cecconi, *Synchronization of non-chaotic ...* Figure 2

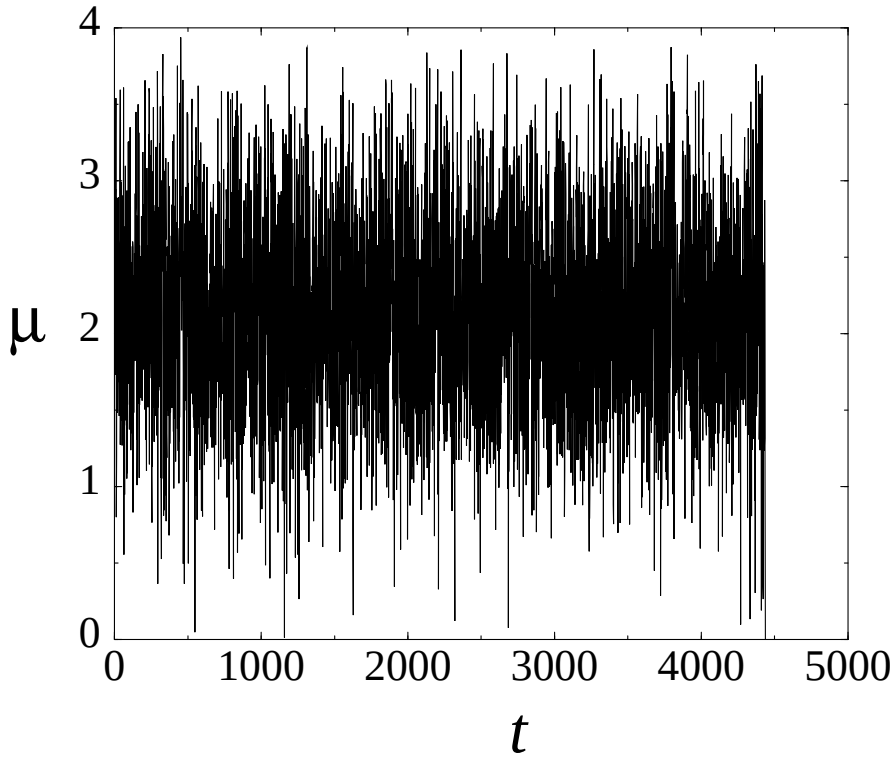
4
3
μ
2
1
0
0
1000
2000
3000
4000
5000
t

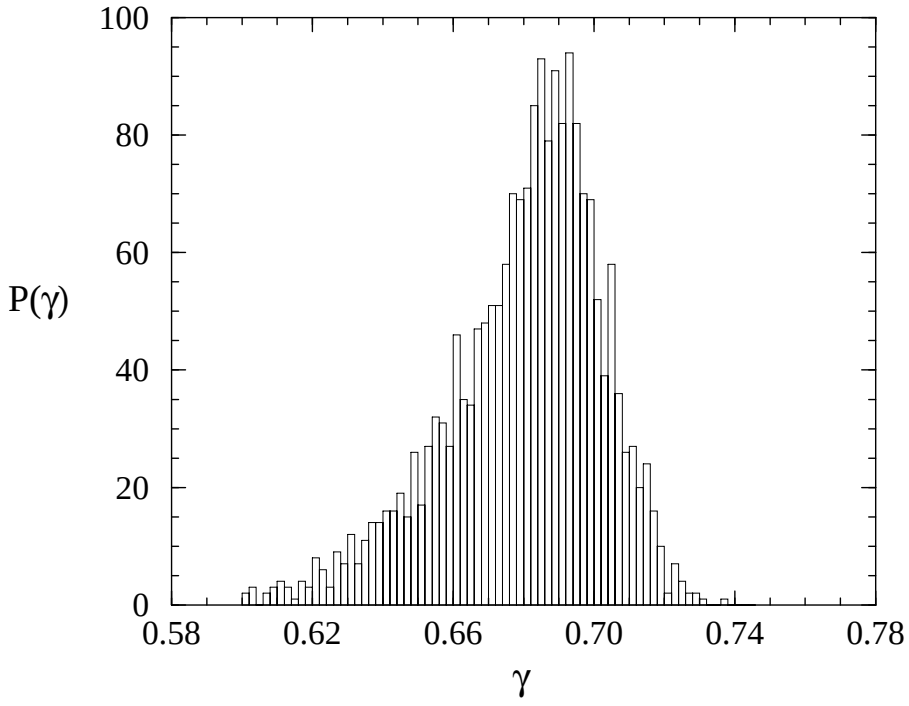

Bagnoli and Cecconi, *Synchronization of non-chaotic ...* Figure 4

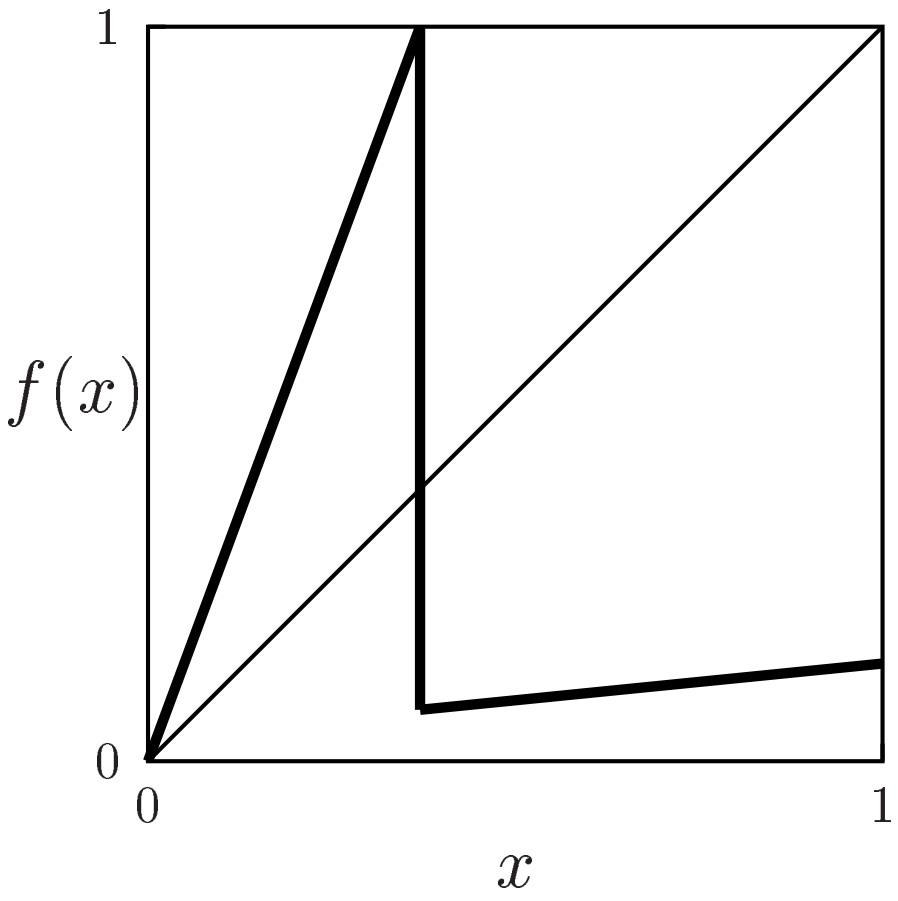

Bagnoli and Cecconi, *Synchronization of non-chaotic ...* Figure 5

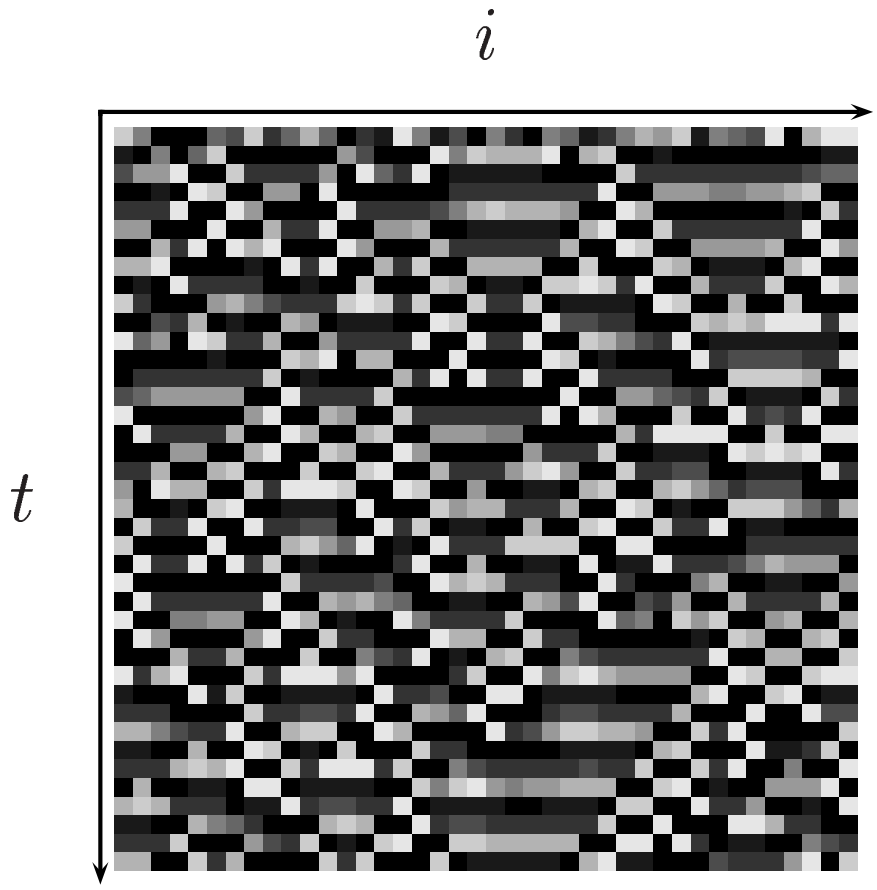
i
t

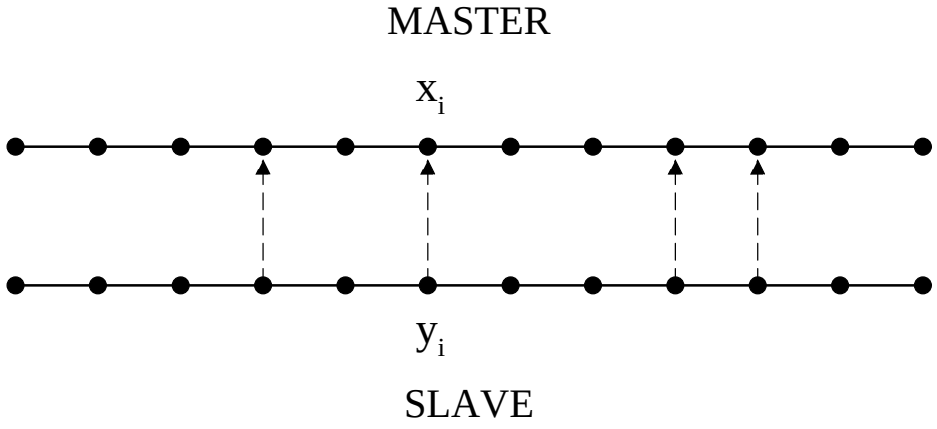
MASTER
x_i
y_i
SLAVE

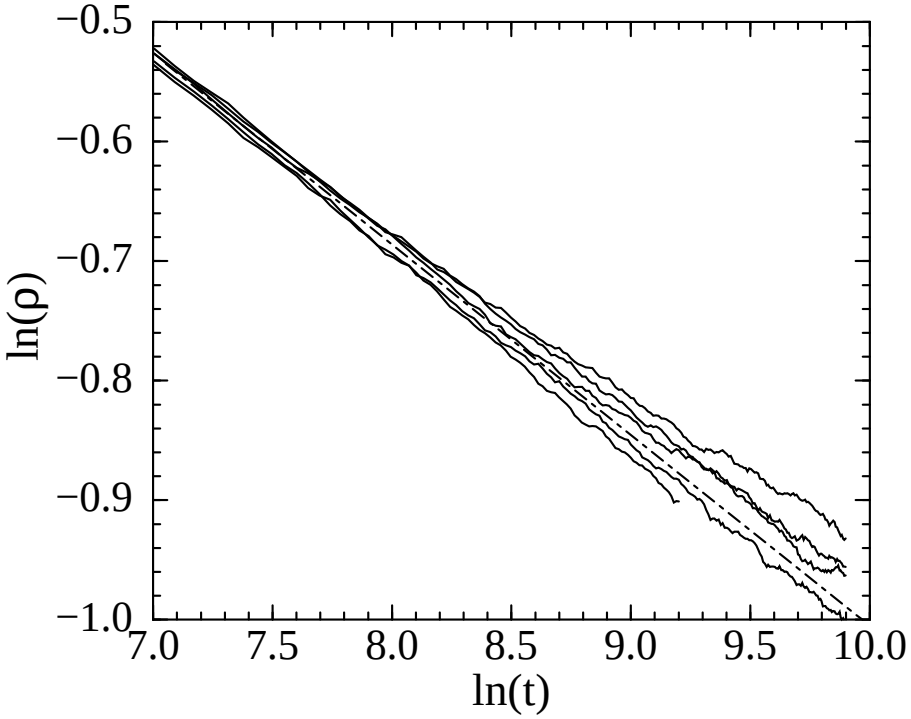

Bagnoli and Cecconi, *Synchronization of non-chaotic ...* Figure 8

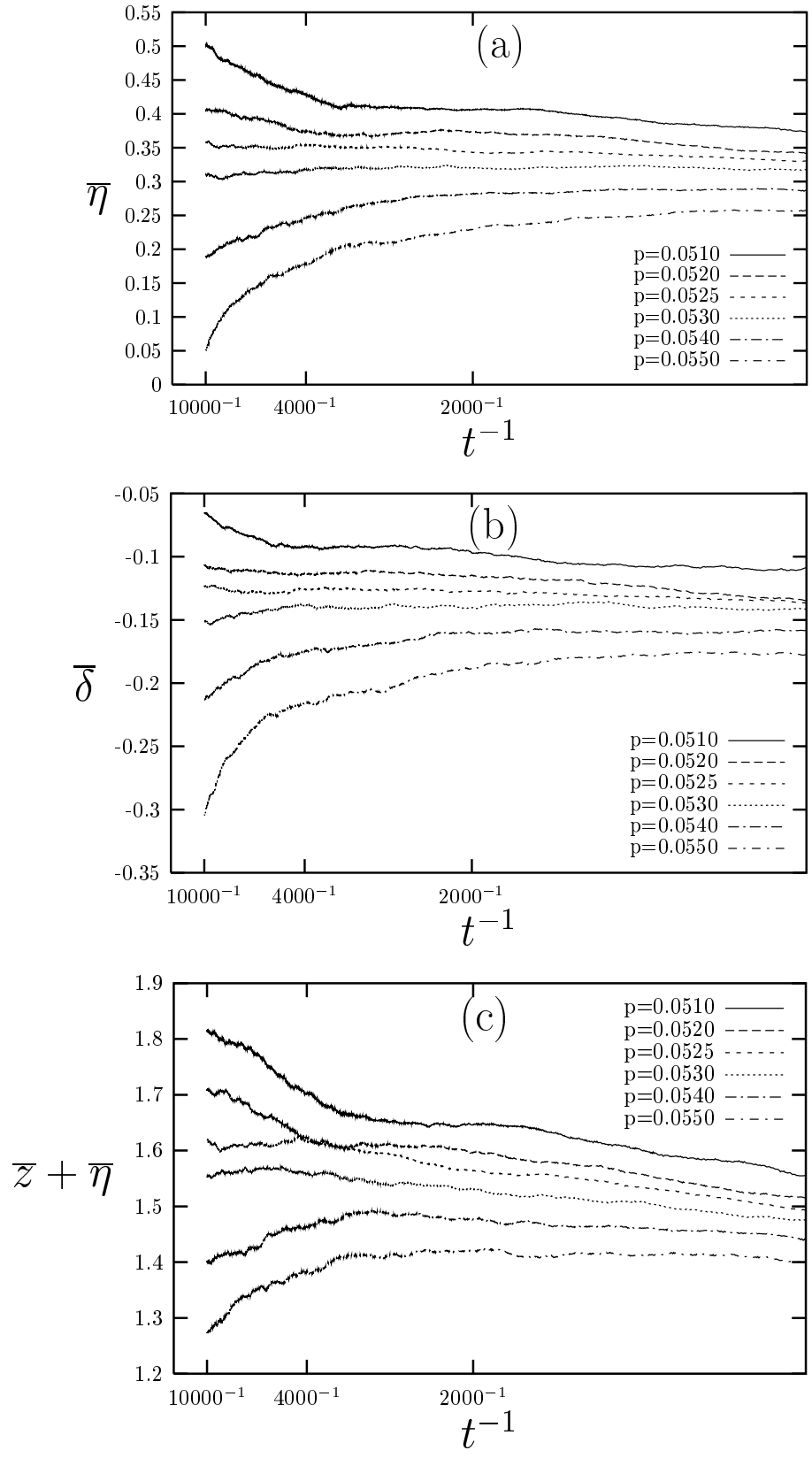

Bagnoli and Cecconi, *Synchronization of non-chaotic ...* Figure 9

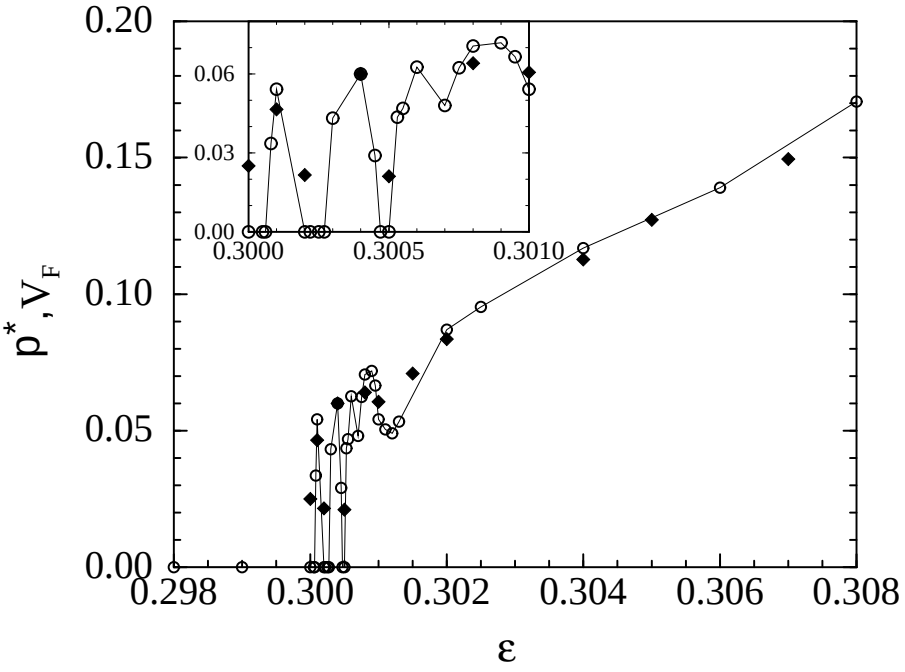

Bagnoli and Cecconi, *Synchronization of non-chaotic ...* Figure 10